Ionospheric Modeling

The Key to GNSS Ambiguity Resolution

Todd Richert and Naser El-Sheimy

THE GPS CARRIER-PHASE OBSERVABLE IS MORE THAN 100 TIMES MORE PRECISE THAN THE CODE-BASED pseudorange observable. Unfortunately, it is also ambiguous. If we want to use the carrier phase as a range measurement in positioning or navigation, we must account somehow for the unknown integer number of cycles or turns of phase in the initial phase measurement when a GPS receiver locks onto a satellite's L1 or L2 signal carrier. Mathematicians, scientists, and engineers have developed clever techniques for helping to resolve these integer ambiguities either in real time or in post-processing collected data. However, the success of these techniques in correctly determining the ambiguities depends on several factors including whether a point or relative positioning technique is employed, the length of the baseline in relative positioning, and how well a variety of errors afflicting the measurements can be mitigated. One source of such errors is the ionosphere. In this month's column, we examine how ionospheric modeling helps in the resolution of carrier-phase ambiguities and how the rate of success in correctly determining the ambiguities will be much improved when GPS observations are combined with those of the future Galileo system. — R.B.L.

One of the major obstacles in resolving ambiguities for longer baselines is the presence of unmodeled ionospheric delays. One technique to deal with this problem is to include ionospheric delay parameters in the observation equations, and estimate them as unknown states.

The purpose of this article is to analyze this technique in light of the future signals that will be available through GPS modernization and the deployment of Galileo. A GNSS software simulator has been used to generate future signals from both GPS and Galileo. These simulated measurements have then been processed by newly developed GNSS processing software to give experimental results showing the effectiveness of ionospheric estimation and how this affects the reliability of ambiguity resolution.

Among other functions, the simulator generates pseudorange and carrier phase measurements from GPS and Galileo satellites. The simulated measurements are corrupted by realistic levels of errors due to the troposphere, the ionosphere, multipath, and thermal noise. Software developed at the University of Calgary in Alberta, Canada, processes these simulated measurements using a Kalman filter. First, a float ambiguity solution is computed, and if desired, the Least Squares Ambiguity Decorrelation Adjustment (LAMBDA) technique is employed to search for integer ambiguities.

TABLE 1 Positioning Scenarios

Scenario	GNSS Type	Measurements Used	
		Carrier Phase	*Code*
GPS2	GPS	L1,L2	C/A, P2
	Galileo	—	—
GPS3	GPS	L1, L2, L5	L2C, L5
	Galileo	—	—
GPS/GAL2	GPS	L1, L5	C/A, L5
	Galileo	E1, E5a	E1, E5a
GPS/GAL3	GPS	L1, L2, L5	L2C, L5
	Galileo	E1, E5a, E5b	E1, E5a

Four Processing Scenarios

For the experiments conducted for this article, four different processing scenarios have been examined.

The first scenario, GPS2, is the current dual-frequency GPS case and will be used as a baseline against which other scenarios will be compared.

GPS3 is the processing scenario of modernized GPS where all three carrier phase measurements (L1, L2, and L5) will be used with L2C and L5 civilian pseudorange codes.

GPS/GAL2 is a scenario using both GPS and Galileo measurements, but only the two shared frequencies of each system (L1/E1 and L5/E5a) are used. This scenario is likely to have applications in the aviation industry because the L1/E1 and L5/E5a bands lie in the reserved Aeronautical Radio Navigation Service frequency band.

Finally, GPS/GAL3 is a dual-system scenario using triple-frequency GPS and triple-frequency Galileo measurements together. Receivers that output all six freely available carrier–phase measurements will probably be more expensive due to the complicated RF front-end and the number of channels required, but they will provide the most redundancy and best accuracy of all the scenarios. The four scenarios are summarized in Table 1.

Ionospheric Delays

In differential GPS, the ionosphere typically has been dealt with in one of three ways: It can be ignored, it can be eliminated using ionosphere-free combinations of dual frequency measurements, or it can be modeled as a state.

Ignoring the Ionosphere. Ignoring the effects of the ionosphere on GNSS measurements is appropriate when the baseline length to be measured is short, and the ionospheric conditions are subdued. In this case, the effect of the (differential) ionospheric delay is negligible and can reasonably be ignored.

Eliminating the Ionosphere. Ionosphere-free combinations of data generally are used for long baselines because the large residual ionospheric effects are virtually eliminated with this combination. Unfortunately, when ionosphere-free combinations of data are used, the measurement noise is greatly increased, and the effective wavelength of the resulting signal is so short that resolving integer ambiguities becomes all but impossible for short observation time spans.

Modeling the Ionosphere. This approach works well for both short and long baselines, and it improves the ability to resolve integer ambiguities. Ionospheric mod-

eling in light of future GNSS signals is the crux of this article.

Ionospheric Estimation

To model the ionospheric delays as a state, an additional parameter for each satellite must be included in the observation equations.

Three Frequencies. For triple-frequency GPS observations, the double-differenced carrier-phase observation equations become:

$$\nabla\Delta\Phi_{L1} = \nabla\Delta\rho - \nabla\Delta dI_{L1} + \lambda_{L1}\nabla\Delta N_{L1} + \varepsilon_{L1}$$
$$\nabla\Delta\Phi_{L2} = \nabla\Delta\rho - \frac{f_{L1}^2}{f_{L2}^2}\nabla\Delta dI_{L1} + \lambda_{L2}\nabla\Delta N_{L2} + \varepsilon_{L2}$$
$$\nabla\Delta\Phi_{L5} = \nabla\Delta\rho - \frac{f_{L1}^2}{f_{L5}^2}\nabla\Delta dI_{L1} + \lambda_{L5}\nabla\Delta N_{L5} + \varepsilon_{L5} \quad (1)$$

where $\nabla\Delta\Phi$ is the double-differenced carrier-phase measurement in meters, $\nabla\Delta\rho$ is the double-differenced geometric range in meters, $\nabla\Delta dI_{L1}$ is the double-differenced slant ionospheric delay in meters on the L1 frequency, λ is the carrier-phase wavelength in meters, $\nabla\Delta N$ is the double-differenced initial ambiguity bias in cycles, f is the carrier-phase frequency in Hz, and ε is the random unmodeled measurement noise.

Pseudo-Observation Equation. For short observation spans, the ionospheric delay is highly correlated with the initial carrier-phase ambiguity because both parameters are effectively constant biases, which cannot be separated without a change in geometry. To alleviate this problem, a pseudo-observation can be used to improve the convergence of the ionospheric delay. The ionospheric pseudo-observation equation is given by

$$\nabla\Delta dI_{pseudo-observation} = \nabla\Delta dI_{L1} \quad (2)$$

where $\nabla\Delta dI_{pseudo-observation}$ is an externally determined value of the expected ionospheric delay.

The pseudo-observation could come from the GPS broadcast ionospheric model, global ionosphere maps, such as those provided by the Center for Orbit Determination in Europe (CODE) analysis center, or it could simply be set to zero. The weighting of this pseudo-observation in the measurement covariance matrix has a significant impact on ambiguity resolution and the accuracy of the final baseline solution.

Weighting the Pseudo-Observable. There are generally three choices of how to weight the ionospheric pseudo-observable:

TABLE 2 Weighting Schemes for the Ionospheric Pseudo-Observable

Variance of Ionospheric Pseudo-Observable	Model Description
$\sigma^2_{pseudo-observable} = 0$	Ionosphere-Fixed
$0 < \sigma^2_{pseudo-observable} < \infty$	Ionosphere-Weighted
$\sigma^2_{pseudo-observable} \to \infty$	Ionosphere-Float

ionosphere-fixed, ionosphere float, and ionosphere-weighted. These three categories are summarized in **Table 2**.

Fixed Model. The ionosphere-fixed model constrains the ionospheric state to a constant value. In short baseline applications when the ionospheric effect is neglected, the ionosphere-fixed model is used implicitly.

Float Model. The ionosphere-float model performs well when long observation time spans are used, but without an external observation, the ionospheric state is highly correlated with the carrier-phase ambiguities causing slow convergence or in some cases divergence of the state vector.

Weighted Model. The ionosphere-weighted model converges more quickly than the float model because it is initially constrained by the ionospheric pseudo-observation. After convergence, the ionospheric states are allowed to change with the changing level of ionospheric activity, which allows the model to fit the observations more accurately.

However, the weighted model has the disadvantage of requiring a suitable variance for the pseudo-observable. Choosing a suitable value for the variance of the pseudo-observation in the ionosphere-weighted model is crucial for reliable ambiguity resolution. For a more detailed explanation of the treatment of ionospheric delays in GPS processing, see Further Reading.

Pseudo-Observable Demo

To demonstrate the effect of the weight of the ionospheric pseudo-observable, we processed a simulated 30-kilometer baseline using different values to weight the ionospheric pseudo-observation. In this test, triple frequency GPS data (L1, L2 and L5) was processed at a sampling rate of 1 Hz.

Figure 1 shows the root-mean-square ionospheric estimation error results for various values of the ionospheric pseudo-observation standard deviation.

The figure clearly shows how the choice of weighting parameter for the ionospheric constraint affects the ionospheric estima-

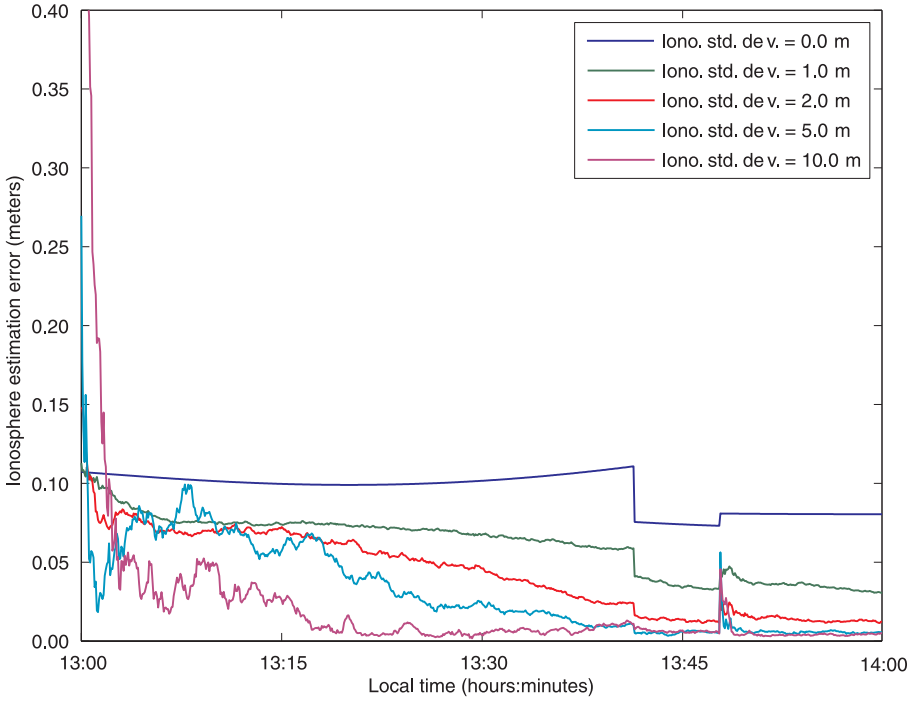

▲ **Figure 1** Ionospheric root-mean-square estimation error using various pseudo-observation standard deviations for a 30-kilometer baseline

tion. The line with the largest standard deviation (magenta), is essentially the float ionosphere model because the float model is, by its nature, a model with a very large standard deviation for the pseudo-observation. This model achieves very poor ionospheric estimation at the beginning of the data set because the ionospheric pseudo-observation is deweighted and the ionospheric estimation relies solely on the noisy pseudorange measurements to observe the ionospheric delay.

As more data is accumulated, the noisy code measurements are filtered and the satellite geometry changes, allowing the ionospheric delays to decorrelate from the carrier-phase ambiguities. After a period of convergence, the float model relies almost exclusively on the more precise carrier-phase data to observe the ionospheric delays, which results in very good ionospheric estimation.

At the other end of the spectrum, the dark blue line (standard deviation of 0.0 meters) gives the results of the ionosphere-fixed model. In this model, the initial ionosphere estimates are better than the initial ionosphere estimates of the float model because the estimates are constrained to zero, which is closer to the true value than the estimate from the noisy code data.

However, as more data is accumulated, the ionospheric estimates are not allowed to converge according to the carrier-phase data because of the tight constraint. This results in the poorest ionospheric estimation at the end of the hour-long data set. The other curves in Figure 1 represent ionospheric standard deviations between zero and 10 meters. These curves demonstrate the impact of using an appropriately weighted ionospheric pseudo-observation: the ionospheric estimation is initially constrained, but relies heavily on the carrier-phase data after a period of convergence.

Changing Satellites. The distinctive step seen in Figure 1 at 13:42 is the result of switching the reference satellite from a lower to a higher elevation angle satellite. There is also an anomaly at 13:47 that is particularly accentuated for the lines with larger ionospheric pseudo-observation standard deviations. This event is the result of a new satellite coming into view. For the cases with the larger standard deviations, the new satellite has more erratic initial estimates, whereas with the fixed and tightly constrained weighted ionosphere model, the initial ionospheric estimation for the new satellite is better.

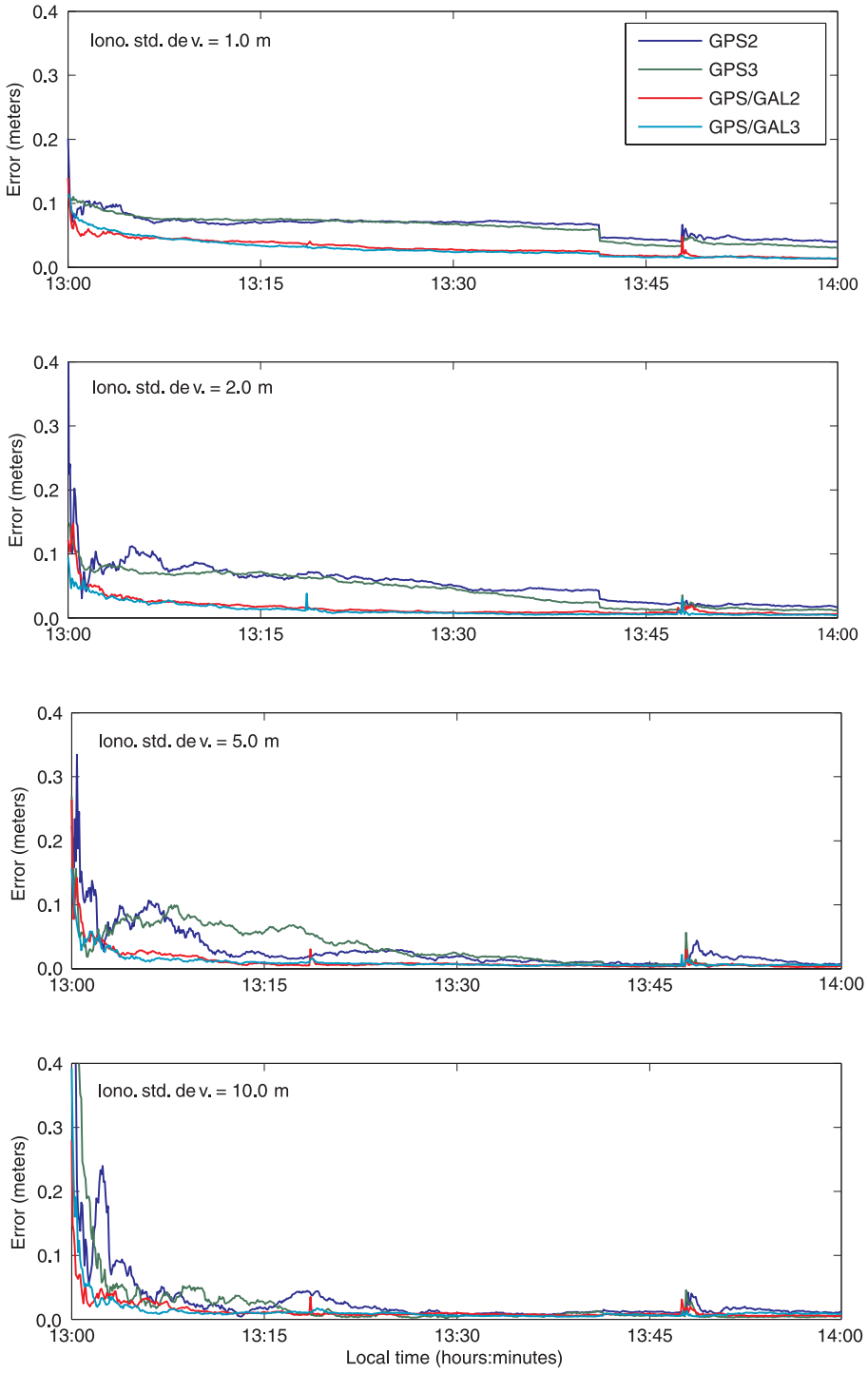

▲ **Figure 2** Ionospheric delay estimation error with various processing scenarios using the weighted ionosphere model

Future GNSS Signals

Future GNSS signals will allow improved ionospheric estimation in three ways. First, if all three available frequencies are used, the ionospheric delay will be more observable. This means that the same parameter (the ionospheric delay on the L1 signal) is observed by three separate carrier-phase observations, increasing the redundancy of the problem.

Second, the future code measurements will be more precise and more resilient to multipath errors than the current C/A-code

and the reconstructed P2-code. Third, when a combined GPS and Galileo system is used, the number of satellites is increased. These three factors enable faster convergence of the ionospheric states.

Figure 2 shows the root-mean-square error of ionospheric delay estimation for the various processing scenarios outlined in Table 1 using the weighted ionosphere model. For all the positioning scenarios, a simulated 30-kilometer baseline in Calgary was processed in kinematic mode with float ambiguities. The observational time span was one hour and the data sampling interval was five seconds. A sampling of values for the ionospheric pseudo-observation standard deviation was used, but in all cases, the actual pseudo-observation was set to zero.

There is a marked difference in the results of positioning scenarios that do and do not use Galileo measurements. Clearly, the increased number of satellites and the precise pseudorange codes will have a significant impact on the ability to estimate the ionospheric delay quickly. Once again, the steps at 13:42 are the result of a reference satellite switch and the small discontinuities seen at 13:47 are from an additional satellite becoming visible.

Ambiguity Resolution

Estimating the ionospheric delay in itself is not useful for positioning applications. The reason for desiring accurate estimates of the ionospheric delays is to enable better estimation of the float ambiguities, which leads to faster, more reliable integer ambiguity fixing and better precision of the baseline components.

To evaluate the ability of each positioning scenario to find the correct set of integer ambiguities, instantaneous ambiguity resolution was attempted every 200 seconds between 7:00 and 22:00 local time in Calgary. In the context of this study, instantaneous ambiguity resolution is defined as ambiguity resolution after only two epochs of 1-hertz data.

Before each attempt at ambiguity resolution, the filter was completely reset so that no *a priori* data was used. This test was conducted during the peak of the diurnal ionosphere cycle. We varied the baseline length from 10 to 80 kilometers and processed the data using all four of the positioning scenarios described in Table 1.

Weighted Model. The weighted ionosphere model was used to estimate the ionospheric delay states and the standard deviation of the ionospheric pseudo-observation was varied from 0.3 to 2.5 meters. The roving receiver was assumed to be kinematic and a medium level of ionospheric activity (for Calgary) was applied to the simulated observations. Since simulated data was used, the correct integer values of the ambiguities are known and the percentage of trials finding this correct ambiguity set are plotted in **Figure 3**.

The first deduction from Figure 3 is that the scenarios that include Galileo measurements find the correct ambiguity set more often than the GPS–only scenarios regardless of the value of the ionospheric pseudo-observation or the baseline length. This result corresponds to the previous plot where it was found that the scenarios using combined GPS and Galileo signals provided more precise estimates of the ionospheric delays.

A second observation from Figure 3 is that the GPS2 and GPS3 scenarios appear to exhibit a distinct maximum in percent of correct ambiguity sets. The maximum is most pronounced for baseline lengths of 10, 20, and 30 kilometers where the maximum values occur at ionospheric pseudo-observation standard deviations of 0, 0.5, and 0.9 meter for GPS2 and 0, 0.7, and 0.9 meter for GPS3. Other investigators have found a similar phenomenon using real dual-frequency GPS data (see Further Reading).

The maximum indicates an optimal balance between weighting the ionospheric pseudo-observation and the code observations. If there is too much weight on the pseudo-observation, the ionospheric delay states are too tightly constrained; whereas, if there is not enough weight on the pseudo-observations, the solution relies too heavily on the code observations and the ionospheric delay states become corrupted by the noise and multipath

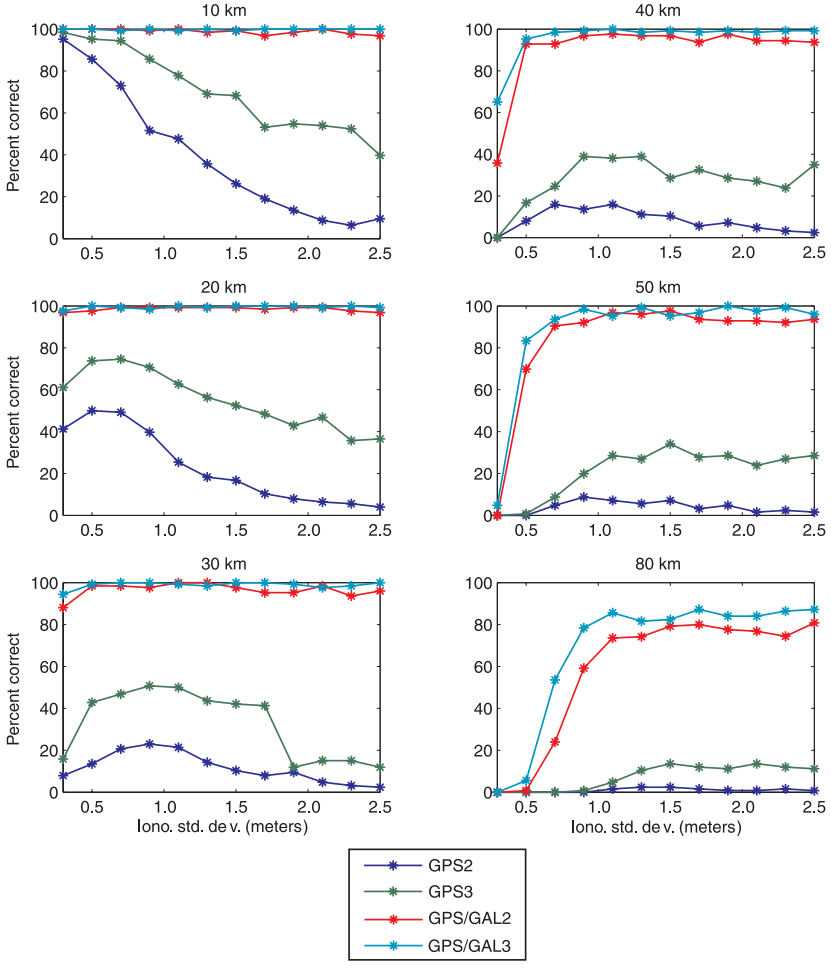

Figure 3 Percentage of correct ambiguity sets versus ionospheric pseudo-observation standard deviation

of the code measurements.

Interestingly, a distinct maximum value is not seen in the cases of GPS/GAL2 or GPS/GAL3. In these positioning scenarios, the percentage of correct ambiguity sets remains fairly constant for a wide range of ionospheric constraint standard deviations. This is understandable when referring back to Figure 2.

GPS + Galileo. When GPS and Galileo are used together, the improved geometry and more precise pseudorange measurements enable very fast and accurate estimation of the ionospheric states. In fact, the ionospheric delay states are estimated so well, that the error in the ionospheric estimation is no longer the factor that limits the ability to find the correct ambiguity set.

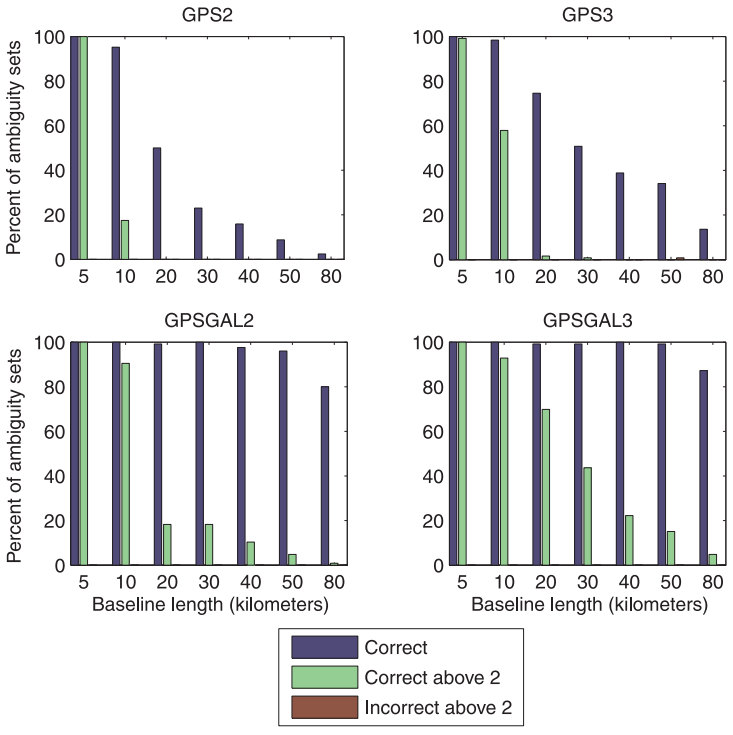

▲ **Figure 4** Instantaneous ambiguity validation as a function of baseline length

Consequently, any improvement in the ability to find the correct ambiguity set resulting from the ionospheric constraint is almost imperceptible. For the 80-kilometer baseline, when the percentage of correct ambiguities is less than 100 percent, the cause is not the error in estimating the ionosphere, but rather, the other unmodeled error sources (that is, residual tropospheric effects). Therefore, the choice of ionospheric pseudo-observation standard deviation is inconsequential as long it does not constrain the ionospheric delays to an incorrect value too tightly.

This analysis illustrates the difficulty in trying to model ionospheric delays as additional unknown parameters for currently available GNSS systems: It is crucial to find an optimal weight for the ionospheric pseudo-observation. However, the problem of finding an optimal value for weighting the ionospheric constraint is essentially eliminated when using GPS and Galileo observations together because an ionospheric pseudo-observation is not needed at all.

Ambiguity Validation. The preceding test examined the ability to find the correct integer ambiguity set. However, the major issue in precise GNSS applications is not only whether or not the correct ambiguity set can be found, but rather whether or not a potential ambiguity set can be successfully validated as correct or incorrect.

Ratio Test. To accomplish the task of validation, a ratio test can be used. In the software used for this study, the ratio that has been implemented is given by:

$$\frac{R_2}{R_1} = \frac{(\hat{a} - K_2)^T Q_{\hat{a}}^{-1} (\hat{a} - K_2)}{(\hat{a} - K_1)^T Q_{\hat{a}}^{-1} (\hat{a} - K_1)} = \frac{\Omega_2 - \Omega_o}{\Omega_1 - \Omega_o} > k \qquad (3)$$

where $\hat{a}$ is the vector of estimated real-valued ambiguities, K_i is the ith potential set of integer ambiguities, $Q_{\hat{a}}$ is the cofactor matrix of the float ambiguities, Ω_0 is the weighted sum of squared residuals from the float ambiguities, subscripts 1 and 2 refer to the best and second best integer ambiguity solutions, and k is some constant value. This test can be understood intuitively as the ratio of the distances between the float ambiguity set and the best and second-best integer ambiguity sets. If the above inequality is true, the best potential set of ambiguities is accepted as the correct one. The constant value, k, is chosen empirically and depends on the desired balance between speed of ambiguity resolution and level of confidence in the ambiguity fixed solution. Other forms of the ratio test exist, but they all require a user-defined constant to indicate the desired level of confidence (see Further Reading).

Effect of Future Signals. To evaluate the effect of future signals on ambiguity validation performance, a test was conducted in which instantaneous ambiguity resolution was performed every 200 seconds during periods of the day that experienced peak ionospheric activity (7:00–22:00 local time).

For this test, we used the ionosphere weighted model to estimate the ionospheric states and we used the optimal ionospheric pseudo-observation standard deviations from Figure 3. The constant value for k in Equation (3) was set to 2.0, which is a commonly used value.

Figure 4 shows the percentage of trials that found the correct ambiguity set (dark blue bars), the percentage of trials that found the correct ambiguity set and generated a ratio value above the threshold of 2.0 (light green bars), and the percentage of trials that did not find the correct ambiguity set, but still had a ratio value above the threshold of 2.0 (burgundy bars).

The preceding figure shows an important feature of using triple frequency data versus dual frequency data. When looking at the 10-kilometer baseline in the GPS2 and GPS3 scenarios, it can be seen that the percentage of correct ambiguity sets that were found is only slightly more for the triple frequency case than for the dual frequency case.

For the GPS3 scenario, 100 percent of the ambiguity sets were correct; whereas, for the GPS2 scenario, 95 percent of the ambiguity sets were correct. However, the percentage of correct ambiguity sets that were successfully validated in the triple frequency case is substantially more than in the dual frequency case. Only 17 percent of the correct ambiguity sets in the GPS2 scenario were successfully validated; whereas, 58 percent of the correct ambiguity sets in the GPS3 scenario were successfully validated.

The same phenomenon is witnessed when looking at the GPS/GAL2 and GPS/GAL3 scenarios. The triple frequency case provides more successful ambiguity validation despite having similar integer ambiguity search performance. The reason for this improvement in ambiguity validation is because the triple frequency scenarios have a greater redundancy than the dual frequency cases. As a result, the correct ambiguity set stands out more clearly as the vector with the smallest distance between the float and fixed ambiguities.

Conclusions

We have shown that there will be significant improvements in the ability to estimate ionospheric delay parameters quickly and precisely when GPS and Galileo observations are used together.

When using only GPS measurements for medium length baselines (10 to 30 kilometers), it is advantageous to use an ionospheric pseudo-observable to constrain the ionospheric delay states to a fixed value. However, one of the difficulties in using an ionospheric constraint is that it is very difficult to find an optimal weight for the constraint equation. This problem is largely avoided when using GPS and Galileo measurements together because improved ionospheric estimation enables one to omit any external constraints.

The best results are obtained when using GPS and Galileo measurements together and estimating the ionospheric delays as unknown parameters without the use of a constraining pseudo-observation.

The use of three frequencies greatly improves the ability to successfully validate correct ambiguity sets compared with dual frequency systems. The additional third frequency for both GPS only and combined GPS/Galileo systems provides only marginal improvement in finding correct ambiguity sets. However, the improved redundancy causes the correct ambiguity set to stand out more clearly as the correct solution when using a ratio test for validation.

Acknowledgments

We would like to acknowledge the financial support of the Natural Sciences and Engineering Research Council of Canada, Waypoint Consulting Inc. (Calgary, Alberta, Canada), and the Alberta Ingenuity Fund, for their generous financial support. This article is a product of a larger research project in the Mobile Multi-Sensor Research Group in the Geomatics Engineering Department at the University of Calgary.

Manufacturers

The GNSS simulator used is based on the *Satellite Navigation TOOLBOX 3.0 For MATLAB* developed by **GPSoft** (Athens, Ohio).

Biographies

TODD RICHERT earned an MSc in geomatics engineering at the University of Calgary in the Mobile Multi-Sensor Research Group under the supervision of Dr. Naser El-Sheimy in 2005. He works for NovAtel Inc. in Calgary, Alberta, Canada, developing real-time kinematic software.

DR. NASER EL-SHEIMY is the Canada Research Chair in Mobile Multi-Sensor Geomatics Systems, and a professor in the Department of Geomatics Engineering at the University of Calgary. He is the chair of the International Federation of Surveyors working group C5.3 on integrated positioning, navigation and mapping systems, the vice chair of the special study group for mobile multi-sensor systems of the International Association of Geodesy, and the chair of the inter-commission working group I/V on "Integrated Mobile Mapping Systems" of the International Society for Photogrammetry and Remote Sensing.

"Innovation" is a regular column featuring discussions about recent advances in GPS technology and its applications as well as the fundamentals of GPS positioning. The column is coordinated by RICHARD LANGLEY of the Department of Geodesy and Geomatics Engineering at the University of New Brunswick, who appreciates receiving your comments and topic suggestions. To contact him, see the "Columnists" section on page 6 of this issue.

Further Reading

For a more detailed explanation of the treatment of ionospheric delays in GPS processing, see

Fast Precise GPS Positioning in the Presence of Ionospheric Delays by D. Odijk, Ph.D. thesis, Dept. of Mathematical Geodesy and Positioning, Delft University of Technology, Delft University Press, Delft, The Netherlands, 2002.

For more on ionospheric modeling for ambiguity resolution, see

"Use of Self-Contained Ionospheric Modeling to Enhance Long Baseline Multiple Reference Station RTK Positioning" by P. Alves, G. Lachapelle, M.E. Cannon, J. Park, and P. Park in *Proceedings of ION GPS 2002*, the 15th International Technical Meeting of the Satellite Division of The Institute of Navigation, Portland Oregon, September 24–27, 2002, pp. 1388–1399.

For the global ionosphere maps produced by the Center for Orbit Determination in Europe (CODE), see

"Global Ionosphere Maps Produced by CODE" a Web page of the Astronomisches Intitut der Universität Bern. <http://www.cx.unibe.ch/aiub/ionosphere.html>

For a report on the proposed preliminary signal formats for Galileo, see

"Status of Galileo Frequency and Signal Design" by G. Hein, J. Godet, J.-L. Issler, J.-C. Martin, P. Erhard, R. Lucas-Rodriguez, and T. Pratt in *Proceedings of ION GPS 2002*, the 15th International Technical Meeting of the Satellite Division of The Institute of Navigation, Portland Oregon, September 24–27, 2002 pp. 266–277.

For information on the LAMBDA ambiguity resolution technique, see

"A New Way to Fix Carrier-Phase Ambiguities" by P.J.G. Teunissen, P.J. de Jonge, and C.C.J.M. Tiberius, in *GPS World*, Vol. 6, No. 4, April 1995, pp. 58–61.

"GPS Carrier Phase Ambiguity Fixing Concepts" by P.J.G. Teunissen, Chapter 8, in *GPS for Geodesy* 2nd Edition, published by Springer-Verlag, Berlin, Germany, 1998, pp. 319–388.

For more on statistical testing for ambiguity validation, see

"Integer Ambiguity Validation: An Open Problem?" by S. Verhagen, in *GPS Solutions*, Volume 8, No. 1, 2004, pp. 36–43.